Sun *et al. Geoenvironmental Disasters* (2024) 11:4
https://doi.org/10.1186/s40677-023-00265-2

Geoenvironmental Disasters

RESEARCH

Open Access

Adsorption performance of bentonite and clay for Zn(II) in landfill leachate

Wen-Jing Sun[1], Qian-Tong Tang[1], Tian-Hao Lu[2], Ri-Dong Fan[1*], Gao-Ge Sun[1] and Yun-zhi Tan[3]

Abstract

Background The increasing prevalence of the Galvanized and dry battery industries has led to a rise in zinc proportions in landfills, posing environmental risks. This study explores the potential of bentonite, renowned for its metal adsorption capability, as a landfill barrier material.

Methods Adsorption characteristics of Zn(II) in natural bentonite and Shanghai clay were investigated. Various factors affecting Zn(II) adsorption, including pH, Na ion strength, contact time, initial Zn(II) concentration, and adsorption temperature, were analyzed through batch-type adsorption tests.

Results The change in pH and Na strength demonstrates no significant impact on the adsorption of Zn(II) onto bentonite, highlighting the strong selectivity of bentonite for Zn(II). Conversely, the equilibrium adsorption capacity of Zn(II) onto clay increases with rising pH or decreasing ion strength. The Zn(II) adsorption onto bentonite is well-described by the pseudo-second-order, intra-particle diffusion, and Elovih models, each achieving an R^2 value exceeding 0.9. While both physical and chemical adsorption coexist in Zn(II) adsorption onto bentonite or clay, the primary determinant of the adsorption rate is chemical adsorption. The adsorption onto bentonite is spontaneous, whereas onto clay it is not. The mechanism involves van der Waals forces, ion exchange, and chemical actions such as inner-sphere complexation for Zn(II) adsorption onto both bentonite and clay.

Keywords Bentonite, Clay, Adsorption, Zn(II), Leachate

Introduction

Zinc industry, alloy forging, zinc-manganese dry battery manufacturing involved in the use of zinc (Sabnavis et al. 2018). As a result, a considerable amount of secondary zinc resources do great harm to the surroundings, which is existing in the landfill as the form of waste (Maung et al. 2019; Rout and Das. 2009). The migration mechanism of pollutants in the barrier is complex, including convection, diffusion, adsorption, and transport by the gaseous (Wu and Wang 2020; Wu et al. 2022; An et al. 2021, 2022a). With the adsorption process controlling their mobility in the soil–water environment (Elbana and Selim 2019). For example, complexation through electrostatic interactions in montmorillonite interlayers (Yang et al. 2019; Caporale and Violante. 2016). Therefore, it is of great significance to study the adsorption mechanism of bentonite.

In recent years, the adsorption of heavy metals, such as Cd(II), Ni(II), Cu(II), Pb(II), and organic pollutant onto clay minerals has been reported (Jiang et al. 2010; An et al. 2022b). However, it is necessary to consider the impact of environmental ions on the adsorption of bentonite. The concentration of Na is found relatively higher in leachate, and generally higher than that of Zn(II) (Negi et al. 2018). Numerous alkali metal ions compete for available sites of adsorbent (Chen et al. 2015), and reduce

*Correspondence:
Ri-Dong Fan
fanrd@dhu.edu.cn
[1] College of Environmental Science and Engineering, Donghua University, Shanghai, China
[2] Shanghai Urban Construction Municipal Engineering (Group) Limited Company, Shanghai, China
[3] College of Civil Engineering and Architecture, China Three Gorges University, Yichang, China

the removal percentage of Zn(II) on adsorbent. At present, there are many studies focusing on the competitive adsorption between heavy metals, but few studies focus on the competitive adsorption between heavy metals and alkali metals such as Na. Therefore, the consideration of the effects of Na on Zn(II) adsorption in clay minerals is necessary.

In addition, the pseudo-second-order kinetic model and intra-particle diffusion model in adsorption kinetic are generally applied to investigate the removal amount of heavy metal (Yuan and Liu 2013). Both of the models are used to analyze the rate-controlling step of the adsorption reaction (Zou et al. 2019). The experimental equilibrium adsorption capacity (Q_e) values are close to the theoretical Q_e values, described by the pseudo-second-order model, indicating that the rate-controlling step of the adsorption process was controlled by chemisorption (Xu et al. 2021). The Elovich equation is one of the most commonly used equations for describing the kinetics of heterogeneous chemisorption (Inyang et al. 2016). It reflects the evolution of adsorbent surface activity throughout the entire adsorption process. The Elovich equation is apt for modeling the kinetics of chemical substance adsorption by natural sorbents (Huang et al. 2012). Therefore, Elovih model was used to model the adsorption of Zn(II) on bentonite and study the Zn(II) heterogeneous adsorption on bentonite. The Langmuir model and the Freundlich model are generally used in adsorption isotherm models (Zhang et al. 2011). The Langmuir model based on the assumption that adsorption to the active sites is independent of the adjacent sites. And the Freundlich isotherm, an empirical model, is applied to represent the multi-layer adsorption on heterogeneous surfaces (Huang et al. 2012; Wang and Guo 2020). The Dubinin–Radushkevich (D–R) model was used to evaluate the average adsorption energy (Es) and to discern the nature of the adsorption process for metal ions, determining whether it corresponds to physical or chemical adsorption. (Matouq et al. 2015; Tohdee et al. 2018).

This study investigated the adsorption performance of GCL bentonite and Shanghai clay for Zn(II). The effects of pH, Na concentration, contact time, initial concentration and temperature on the adsorption performance are obtained by batch-type adsorption tests. The adsorption kinetic model employs the pseudo-second-order model, intra-particle diffusion model, and Elovich model. The adsorption isotherm models involve the Langmuir model, Freundlich model, and D–R model. The temperature dependence and spontaneity of the adsorption process are analyzed by adsorption thermodynamics (Zou et al. 2019). The adsorption mechanisms of bentonite and shanghai clay are studied by scanning electron micrograph (SEM), X-ray energy dispersion spectroscopy (EDS) and fourier transform infrared spectroscopy (FTIR).

Materials and methods

Materials

Bentonite is obtained from Geosynthetic Clay Liner (GCL) in common landfill, and clay is obtained from Shanghai, China. The main physical properties of the bentonite and clay were tested as per ASTM D4318-10, as shown in Table 1. The specific surface area of bentonite is larger than that of clay, which can produce more adsorption sites. The value D_{97} represents the particle diameter below which 97% of the particles by mass are included in a particle size distribution. This value clay is lower than that of bentonite, indicating that the heavy metals are more likely to migrate between clay particles (Huang et al. 2020).

Reagents

In this study, the reagents of $ZnCl_2$ and NaCl were used to provide Zn and Na respectively, which were purchased from Sinopharm Chemical Reagent Co. Ltd. (China). All reagents were analytical grade. And the solutions were prepared with deionized water (DI water) and stored at 4 °C.

Batch-type adsorption experiments

Adsorption effect parameter

The test scheme and parameters in this study are shown in Table 2. The pH value and the temperature are determined by parameters of common landfill (Szymanski et al. 2018). The control group was established with a pH of 7, Na concentration of 0 mg/L, Zn(II) concentration of 400 mg/L, a test duration of 1440 min, and a temperature of 22 °C.

The experimental procedures followed the method in ASTM D4646. (1) Bentonite and clay were air-dried, grinded and sieved through a 200-mesh screen separately. (2) A Zn(II) solution of the desired concentration was prepared, and the pH was measured by a pH meter.

Table 1 Physical properties of bentonite and clay

Physical property	Bentonite	Shanghai clay
Liquid limit, w_L (%)	153.4	35.98
Plastic limit, w_p (%)	26.80	22.2
Specific surface area, (m^2/kg)	697.5	631.6
Relative density, d_s	2.71	2.67
Cation exchange capacity, *CEC* (meq·100 g^{-1})	68	N.D
D_{50} (μm)	6.46	7.32
D_{97} (μm)	94.93	45.53

Table 2 The scheme of batch-type adsorption test

Experiment number	Solid mass	Liquid volume	$ZnCl_2$ concentration	NaCl concentration	pH	Contact time	temperature
	g	ml	mg/L	mol/L		min	°C
1	3	60	400	0	7	1440	22
2			100	0	7	1440	22
3			200				
4			300				
5			500				
6			600				
7			400	0.001	7	1440	22
8				0.01			
9				0.1			
10			400	0	3	1440	22
11					4		
12					5		
13					6		
14					8		
15			400	0	7	5	22
16						10	
17						15	
18						30	
19						60	
20						120	
21			400	0	7	1440	30
22							40
23							50

(3) A 250 mL conical flask containing 3 g adsorbent and 60 mL Zn(II) solution with a given concentration. (4) The mixture was shaken at a given temperature and for a specific duration in a vibrator. (5) Subsequently, it was centrifuged at 7500 r/min for 20 min, and the supernatant was filtered. The equilibrium concentration of Zn in the liquid was determined using ICP.

Residual concentration of Zn(II) in solution

After the adsorption experiment, the extract was centrifuged for 20 min at a speed of 7500 r/min. The concentration of Zn(II) in the centrifugal liquid is analyzed using a inductively coupled plasma spectrometer (ICP). Each mean was based on at least three analyses, repeated until its relative standard deviation was less than 5%.

Characterization analysis

To understand microstructure and changes of element content of adsorbent sample, the sample of adsorbents No. 1 are characterized by scanning electron microscope (SEM), X-ray energy dispersion spectroscopy (EDS), Fourier transform infrared spectra (FTIR).

Scanning Electron Microscope (SEM) (S-4800, Japan) are used to determine the structure of adsorbent. Fourier Transform Infrared Spectra (FTIR) spectra are measured using KBr pressed disk technique. Bruker AXS Microanalysis GmbH Berlin (Germany) are used to investigate the change of element of adsorbent.

Result and discussion

Figures 1, 2, 3, 4, 5, 6, 7, 8, 9, 10 and 11 shows the equilibrium adsorption capacity q_e or the instantaneous adsorption capacity q_t of the effect of initial pH_0, concentration of Na, contact time, initial Zn(II) concentration and temperature on Zn(II) adsorption by bentonite or clay. In addition, the equilibrium adsorption capacity q_e, the instantaneous adsorption capacity and the removal percentage can be determined in Eqs. (1)–(3):

$$q_{\mathrm{e}} = \frac{C_0 - C_{\mathrm{e}}}{m_{\mathrm{s}}} V \tag{1}$$

$$q_{\mathrm{t}} = \frac{C_0 - C_{\mathrm{t}}}{m_{\mathrm{s}}} V \tag{2}$$

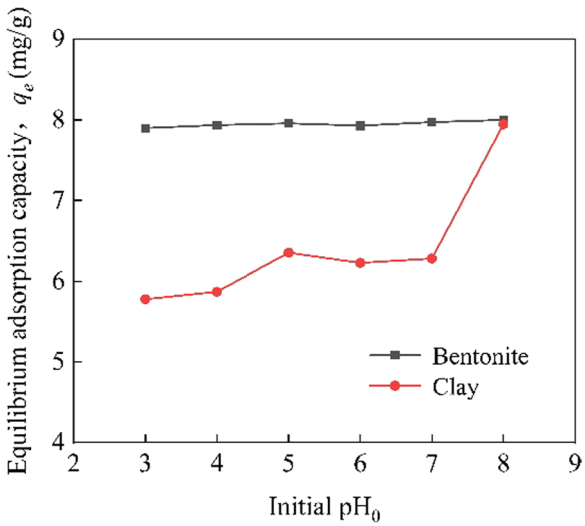

Fig. 1 The effect of initial pH$_0$ on equilibrium adsorption capacity q_e

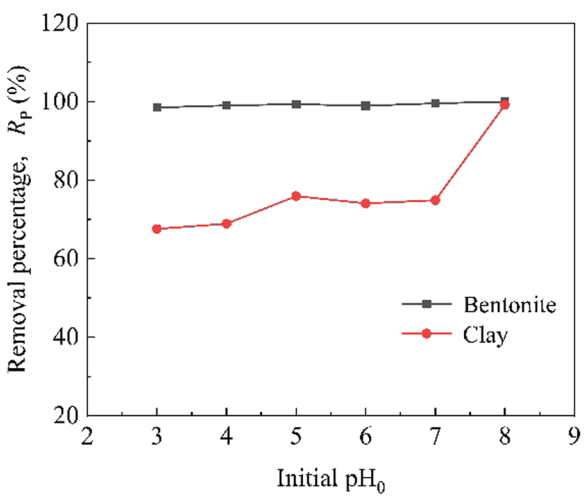

Fig. 2 The effect of initial pH$_0$ on removal percentage R_P

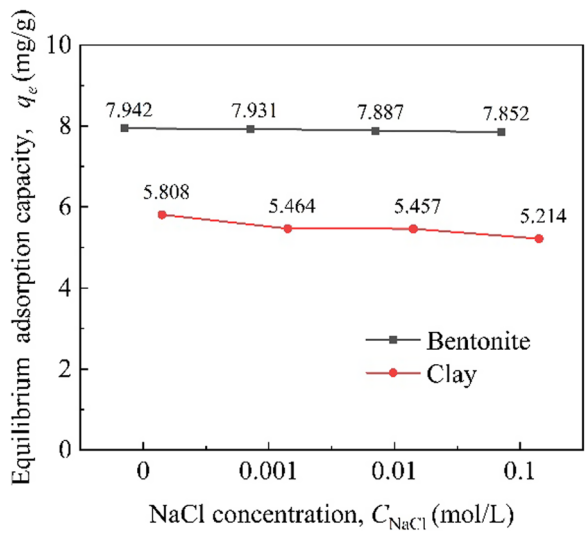

Fig. 3 The effect of Na concentration on equilibrium adsorption capacity q_e

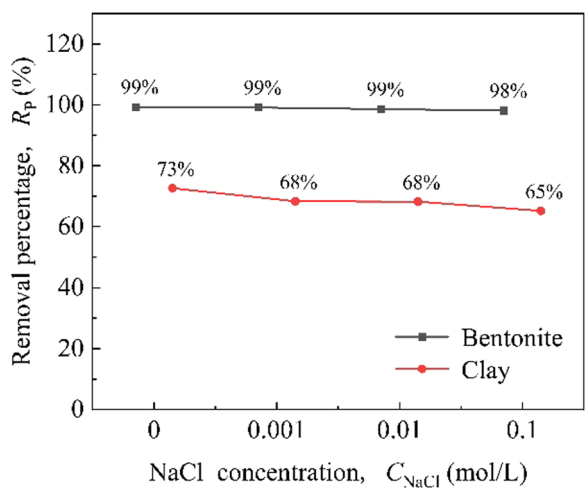

Fig. 4 The effect of Na concentration on removal percentage R_P

$$R_P = \frac{C_0 - C_e}{C_0} \times 100\% \tag{3}$$

where q_e is correspond to the adsorption capacities at equilibrium (mg/g); q_t is the adsorption at time t (mg/g); C_0 and C_e correspond to the concentration of solute at initial and equilibrium respectively (mg/L); m_s is the mass of adsorbent (g) and V is the volume of solution.

As shown in Figs. 1 and 2, the adsorption of Zn(II) by bentonite is not change obviously with the solution pH increase from 3 to 8, which stays stably in the range of 7.9–8.0 mg/g. It appears that the value of pH which range of 3–8 does not significantly impact the adsorption of Zn(II) onto bentonite, the Zn(II) removal percentage exceeds 99%. In contrast, the value of q_e for Zn(II) adsorption onto clay increases from 5.78 to 6.22 mg/g as the solution pH increase from 3 to 7. And it increases greatly when the pH is 8, indicating that there were other factors impact the Zn(II) removal percentage onto clay at the pH range of 7–8.

The heavy metal adsorption from leachate is usually carried out in the presence of other ions, such as Na. Figure 3 and 4 show the change of q_e and R_p on bentonite and clay adsorption Zn(II) with the change of Na concentration. The increase of Na concentration from 0.001 to 0.1 mol/L resulted in an obvious decrease of Zn(II) onto bentonite and clay from 7.94 and 5.81 mg/g to 7.85 and 5.21 mg/g, which decreased by 1.13% and

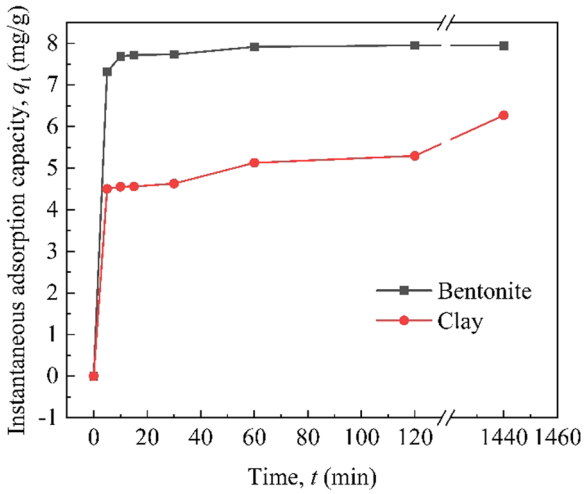

Fig. 5 The effect of contact time on instantaneous adsorption capacity q_t

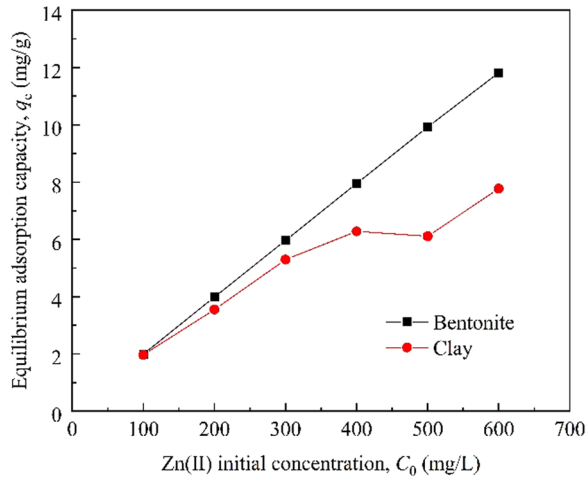

Fig. 7 The effect of Zn(II) initial concentration on equilibrium adsorption capacity q_e

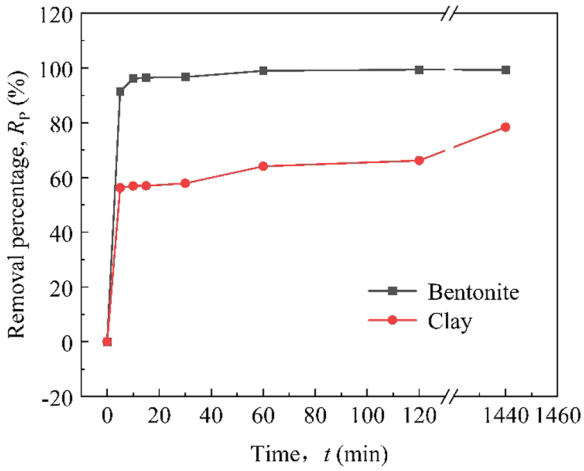

Fig. 6 The effect of contact time on removal percentage R_p

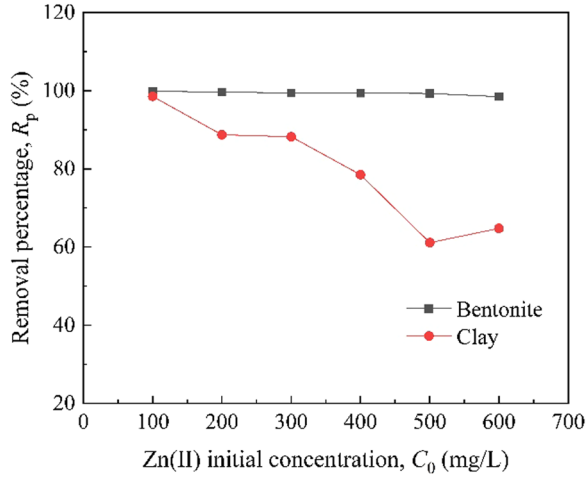

Fig. 8 The effect of Zn(II) initial concentration on removal percentage R_p

10.33%, respectively. The results indicate that the presence of Na has few effects on the removal of Zn(II) onto bentonite, but that weakens the removal percentage of Zn(II) onto clay.

The relationship of the Zn(II) adsorption capacity q_t and time t is shown in Fig. 5 and 6. At 11 min, both bentonite and clay reach a significant level of q_t for Zn(II), with bentonite exhibiting a higher q_t than clay. Between the time interval of 11 and 1440 min, bentonite consistently maintains a high level of adsorption capacity (qt) for Zn(II). In contrast, clay requires a more prolonged duration to achieve a specific instantaneous adsorption capacity. For instance, the qt of clay gradually increases from 4.5 to 6.3 mg/g at 1440 min. In comparison, the instantaneous adsorption capacity of bentonite reaches 6.3 at approximately 5 min. This observation suggests that the clay barrier facilitates a more pronounced migration of Zn(II) toward the perimeter of the landfill.

Figure 7 and 8 show the effect of the initial concentration of Zn(II) on the Zn(II) equilibrium adsorption capacity (q_e) and removal percentage (R_p). It appears that the increase in C_0 does not affect the removal of Zn(II) by bentonite, and the value of q_e increases linearly with the increase in the C_0 value. This indicates that the great amount of available adsorption sites of bentonite ensure that the sites remain, which have not yet been occupied by Zn(II). Then, the amount of adsorbed Zn(II) by clay slowed down or even decreased with the value of C_0 increased from 100 to 500 mg/L, indicating

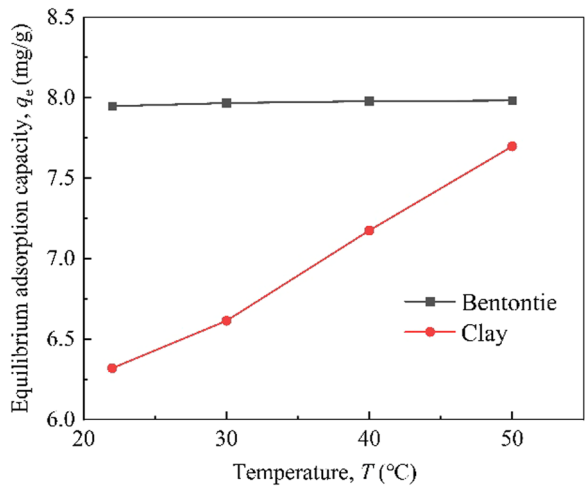

Fig. 9 The effect of temperature on equilibrium adsorption capacity q_e

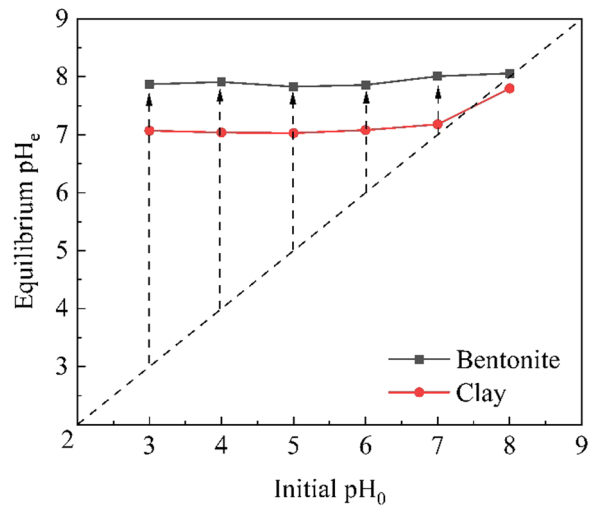

Fig. 11 The relationship between the pH_e after adsorption equilibrium and the initial pH_0

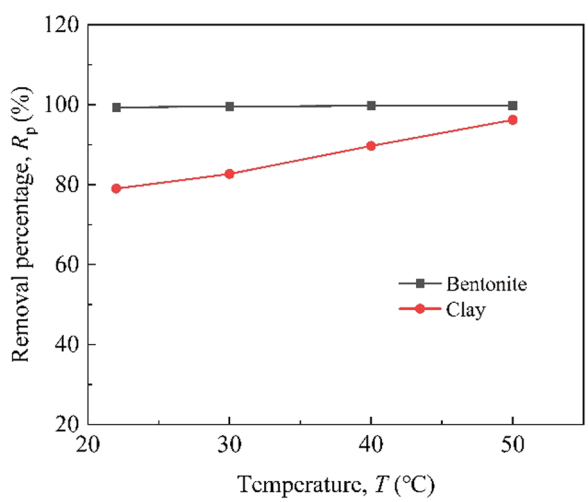

Fig. 10 The effect of temperature on removal percentage R_p

that saturation or equilibrium between Zn(II) and clay likely to achieved.

Figure 9 and 10 show the effect of temperature on the q_e and R_p of Zn(II) adsorbed by adsorbent. Increasing temperature has a positive effect on the adsorption of Zn(II) onto bentonite and clay, especially on clay.

Effect of pH on Zn(II) adsorption

The pH of solution is greatly important to removal of Zn(II) onto bentonite and clay. This is attributed to the influence of solution pH on the structure of clay minerals, and consequently impacting their metal-binding capabilities (Hao et al. 2019).The pH of solution has a slight impact on the adsorption of Zn(II) onto bentonite indicating the affinity of Zn(II) to the adsorption sites on the surface of adsorbent so that bentonite remove Zn(II) stably. However, the pH of the solution seems to has a great impact on the adsorption of Zn(II) onto clay, because the surface of the adsorbents is likely to be covered by H^+ while the pH is low (3–7 in this experiment) (Niu et al. 2020). This phenomenon leads to the competition between the H^+ and Zn(II) and increasing the positive charge density, which repulsed with Zn(II), on the surface of clay (Zhang et al. 2019). It resulting that the clay demonstrated low adsorption capacity toward the removal Zn(II) in solution. The increases of Zn(II) adsorption on clay in alkaline solution (pH 8) is explained due to the adsorption sites on the surface and the edge of amphoteric crystals are deprotonated, and the electrostatic repulsion on surface is weakened (Mahmoud. 2013). In addition, the formation of hydroxide precipitation ($Zn(OH)_2$) (Eqs. 4, 5) is the other reason of the increase of adsorption capacity in clay(Chai et al. 2017).

$$Zn^{2+} + H_2O \rightarrow Zn^{+} + H^{+} \tag{4}$$

$$Zn^{+} + H_2O \rightarrow Zn(OH)_2 \downarrow + H^{+} \tag{5}$$

To understand the effect of adsorbent on the pH in leachate as the process of adsorption, the pH of solution on bentonite and clay adsorbed Zn(II) for 1440 min was tested, as shown in Fig. 11 The final pH of solution around 8 and 7 in equilibrium of adsorption by bentonite and clay respectively, indicating that bentonite may have a neutralizing effect on the acidic solution compared to clay. Increase in the final pH in

solution may be attributed to the replacement of alkaline metals (such as Na, K) with Zn(II) in interlayer of bentonite and clay. Alkali metals are more reactive than Zn(II); therefore, the displacement of alkali metals by Zn(II) results in an increase in solution pH. The increase in the final pH of the solution can be attributed to the substitution of alkali metals (such as Na, K) with Zn(II) within the interlayers of bentonite and clay. Alkali metals are more reducing than Zn(II); consequently, the displacement of alkali metals by Zn(II) leads to an increase in solution pH. Furthermore, the dissolve of carbonate, it presented in the structure of natural bentonite, may be another reason (Jiang et al. 2016; Wang et al. 2020). Then, Zn(II) may form complexes with OH^- at 8 pH in solution, as a result involving in the adsorption and precipitate onto the bentonite structure.

Effect of Na concentration on Zn(II) adsorption

In practice, the composition of landfill leachate is complex, and the adsorption of Zn(II) on the barrier is generally accompanied by the interfering ions, such as Na. Generally, the cation exchange in interlayer is place in saturate exchange sites via exchange H^+ and Na^+ (Chen et al. 2012). However, the bentonite shows higher selectivity of Zn(II) rather than the clay (the removal percentage remains above 98%) as the Na ionic strength increased from 0 to 0.1 M, it indicating that the exchange site in interlayer of bentonite may unsaturated. This conclusion supported by the fact that the exchange sites in clay saturate faster because the clay has a lower cation exchange capacity than the bentonite, as a result the amount of Zn(II) adsorbed on clay decreased with the increase of Na ionic strength (Musso et al. 2019).

Effect of contact time and adsorption kinetics

To determining the equilibration rate in adsorption experiment with contact time, pseudo-second-order model (Eq. 6), intra-particle diffusion model (Eq. 7) and Elovih model (Eq. 8) are used to fit the adsorption kinetic curves of bentonite and clay.

$$\frac{t}{q_t} = \frac{1}{K_2 q_e^2} + \frac{1}{q_e} t \tag{6}$$

$$q_t = k_{int} t^{0.5} + C \tag{7}$$

$$q_t = \frac{1}{\beta} \ln (1 + \alpha \beta t) \tag{8}$$

where q_e is the Zn(II) adsorption capacity at equilibrium (mg/g); q_t is the Zn(II) adsorption capacity at time t (mg/g), while t is the contact time; K_2 is the adsorption constants of pseudo-second-order; Kinetics is the rate constants of intra-particle diffusion; C is the intercept, which is related to the boundary layer thickness.

The correlation coefficients of three models are shown in Table 3. The pseudo-second-order model is best conform to the adsorption of Zn(II) onto bentonite and clay, because it affords a high correlation coefficient ($R^2 > 0.99$), and it obtains a q_e value similar to the equilibrium adsorption capacity determined by indoor experiments. It indicating that the rate limiting step of adsorption process is controlled by chemical adsorption instead of physical adsorption (Song et al. 2019; Xia et al. 2019). The adsorption of Zn(II) onto bentonite and clay primarily be attributed to chemical adsorption through electrons exchange in interlayer of adsorbents (Niu et al. 2020). The higher efficiency, which the value of K_2 for the adsorption onto bentonite and clay is 0.224 and 0.074 respectively, in uptake of Zn(II) onto bentonite, it may relate to the specific surface area of two adsorbents. Furthermore, their adsorption rate is a reflection of the affinities of adsorbents to Zn(II), obviously, bentonite has a higher affinity to Zn(II) (Elbana and Selim 2019).

The Elovich model is also a suitable kinetic equation for describe the adsorption of Zn(II) onto bentonite and clay. The value of R^2 is >0.99 for two adsorbents, which indicating that the bentonite and clay are heterogeneous nature. Furthermore, the diffusion might be the rate limiting step in addition to chemical adsorption (Bagherifam et al. 2021), which can be confirmed by the intra-particle diffusion. If a plot of the amount of adsorbate adsorbed per unit weight of adsorbent, q_t, vs. square root of contact time not gives a linear plot (as shown in Fig. 12), it indicates that

Table 3 The kinetic model constants and correlation coefficients for Zn(II) adsorption onto bentonite and clay

Adsorbent	Pseudo first–second model			Intra-particle diffusion model			Elovih model		
	q_e	K_2	R^2	K_{int}	C	R^2	α	β	R^2
	mg/g	g/(mg min)		mg/(g^{-1}/min$^{-0.5}$)					
Bentonite	7.987	0.224	0.999	0.037	7.572	0.906	7.982×10^{16}	5.673	0.999
Clay	5.376	0.074	0.999	0.101	4.15	0.926	6.338×10^{5}	3.731	0.994

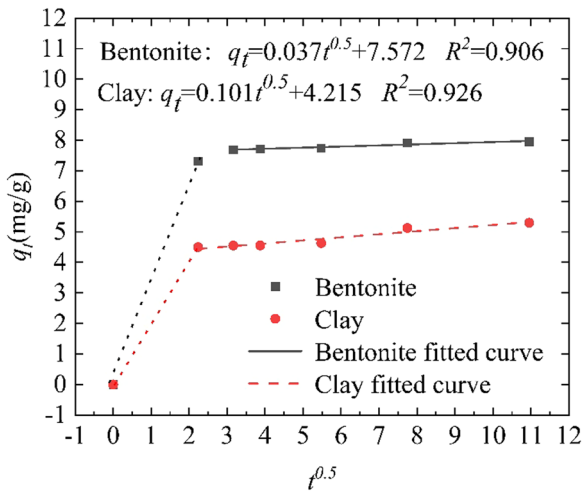

Fig. 12 Intraparticle diffusion plots for Zn(II) adsorption onto bentonite and clay

intraparticle diffusion is the rate-limiting step but not the singular (Albadarin et al. 2012).

Effect of initial concentration and adsorption isotherm

The initial solute concentration effects the resistance of mass transfer between the liquid and the solid, and effect the chemical adsorption, such as cation exchange, of heavy metal onto adsorbents. To characterize the adsorption performance of Zn(II) onto bentonite and clay, and to gain insights into the affinity between adsorbates and adsorbents, the Langmuir, Freundlich, and D–R isotherm models were employed.

The Langmuir model is an ideal model independent of adsorption capacity or coverage, which have shown to be suitable for describing the monolayer adsorption on a homogeneous surface (Eq. 9) (Chang et al. 2020). The Freundlich model is based on un surface (Eq. 10). The D–R model assumed the adsorption process of adsorbent filling the adsorbent hole (Eq. 11).

$$q_e = \frac{K_L q_m C_e}{1 + K_L C_e} \tag{9}$$

$$q_e = K_F C_e^{1/n_F} \tag{10}$$

$$q_e = q_m \exp\left(-K_{DR}\varepsilon^2\right) \tag{11}$$

where q_e and q_m is the adsorption capacity at equilibrium and the maximum adsorption capacity respectively(mg/g), C_e is the equilibrium concentration of solution, K_L and K_F is the contents of Freundlich which is a direct measure, n_F is the index of anisotropy.

As shown in Table 4, Freundlich model have shown to be most suitable for describing the adsorption on bentonite in three models, because it affords a high correlation coefficient (R^2=0.973). the value of $1/n_F$ is 0.1–1 indicating a favorable adsorption (Dinh et al. 2022). The $1/n_F$ of adsorption of Zn(II) onto bentonite and clay is 0.452 and 0.263 respectively, representing a favorable Freundlich adsorption on bentonite and clay. In Table 4, the process of the bentonite adsorption of Zn(II) is also conforms to the Langmuir model and D–R model, both of which determine correlation coefficients greater than 0.95. Thus, the adsorption of Zn(II) by bentonite includes both homogeneous process on the surface in a monomolecular layer and pore filling processes. This ensures stable adsorption of Zn(II) onto bentonite, as a result in Fig. 1h. The two models determined similar q_m values, indicating that the maximum adsorption capacity of bentonite at 6031.3 K (22 °C) is about 14 mg/g. The *Es* presents the average adsorption free energy, which is calculated from k_d. The *Es* value of Zn(II) adsorption onto bentonite and clay is 10.526 kJ/Mol and 8.772 kJ/Mol, respectively. According to Zou et al. (2019), this value is in the range of 8–16 kJ/Mol indicated the process of adsorption controlled by chemical mechanisms, such as surface complexation.

Effect of temperature and adsorption thermodynamics

The spontaneity of adsorption of heavy metals onto adsorbents are indicated by adsorption thermodynamics. The Van't Hoff plot of $\ln K_d$ versus T is shown in Fig. 13, which reflect the temperature dependence of removal rate. The values of thermodynamic parameters ΔH, ΔS, ΔG obtained are listed in Table 5, which confirmed by Eqs. (12)–(14):

Table 4 Adsorption isotherm constants values for Zn(II) adsorption onto bentonite and clay

Adsorbents	Langmuir model			Freundlic model			D–R model		
	q_m mg/g	K_L L/mg	R^2	K_F mg/g	$1/n_F$	R^2	q_m mg/g	*Es* kJ/Mol	R^2
Bentonite	13.755	0.625	0.972	4.858	0.452	0.973	14.088	10.526	0.964
Clay	7.391	0.068	0.955	1.785	0.263	0.925	5.958	8.772	0.831

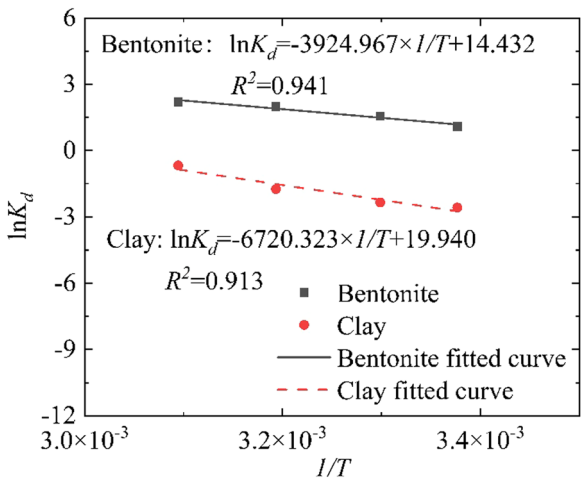

Fig. 13 The Van't Hoff plot of lnK_d versus T

Table 5 Thermodynamic parameters for Zn(II) adsorption onto bentonite and clay

Adsorbents	*T* K	*ΔH* kJ/mol	*ΔS* J/(mol K)	*ΔG* kJ/mol	R^2
Bentonite	295.15	32.64439	119.3796	−2.70988	0.941
	303.15			−3.54553	
	310.15			−4.73933	
	323.15			−5.93312	
Clay	295.15	56.43134	166.8304	7.024507	0.913
	303.15			5.856694	
	310.15			4.18839	
	323.15			2.520085	

$$\Delta G = \Delta H - T \cdot \Delta S \tag{12}$$

$$K_{\mathrm{d}} = \frac{C_0 - C_{\mathrm{e}}}{C_{\mathrm{e}}} \cdot \frac{V}{m} \tag{13}$$

$$\ln K_{\mathrm{d}} = \frac{\Delta S}{R} - \frac{\Delta H}{RT} \tag{14}$$

where ΔS is the entropy, ΔH is the enthalpy, ΔG is the Gibbs free energy, K_{d} is the adsorption equilibrium constant, R is the constant of gas, which value is 8.314 J mol^{-1} K^{-1}.

The ΔH reflects the energy barrier of adsorption (Xu et al. 2021). Generally, the adsorption process is considered physical when the absolute magnitude of the adsorption heat is less than 25 kJ/mol and chemical when it exceeds 40 kJ/mol (An et al. 2022b). The adsorption heat of Zn(II) on bentonite is measured at 56.43 kJ/mol, indicating a chemical adsorption process for Zn on bentonite. The increasing temperature, which involves the rise of adsorption capacity and decreasing in the retarding forces acting on the diffusing ions (Ahmed et al. 2021), favored the chemical reaction between adsorbents and adsorbate. In addition, the randomness at solid/solution interfaces reflected by ΔS. The ΔS during the Zn(II) adsorption onto bentonite and clay is 119.38 J/(mol K) and 116.83 J/(mol K) respectively, indicating that the affinity of bentonite and clay toward Zn(II) (Yao et al. 2014).

The ΔG confirm the difference of adsorption capacity on bentonite and clay. The Zn(II) adsorption onto bentonite can be spontaneous ($\Delta G < 0$), which is different from the study by Chai et al. (2017). In contrast, it is difficult to adsorb Zn(II) spontaneously onto clay, which is consistent with the phenomenon in Fig. 1i.

Adsorption mechanism

To understand the adsorption mechanism of bentonite and clay toward Zn(II), SEM、FTIR and EDS are usually analysis to performed the adsorbents before and after adsorption. The conditions of adsorption are given, which pH 7, temperature is 22 °C, the Zn(II) concentration is 400mg/L, the contact time is 1440 min, No Na interference.

The SEM images of the original and Zn(II)-adsorbed adsorbents are shown in Figs. 14 and 15. The original images of bentonite, as shown in Fig. 14, shows a fine, slice-like structure, with the folds on the surface, which is the character of montmorillonite. The slice-like morphology is an important factor effecting the adsorption performance (Xia et al. 2019). The clay mineral shows an irregularly heterogeneous and there is a presence of smaller grains on surface (Sihombing et al. 2018). The surfaces of both minerals become rough after Zn(II) adsorption (Fig. 15), which is similar to the results gained by Liu et al. (2017). The images of bentonite shows a collapsed skeleton after Zn(II) adsorption. It appears that the morphological changes of clay surface are more aggregated and the formation of the large clumps. It attributed that the negative surface of clay is partially neutralized by positively charged Zn(II), which reduced the repulsion of clay particles (Chai et al. 2017).

As can be seen from the result reported in Table 6, the chemical composition changes of absorbents before and after adsorption can be analyzed by EDS, such as soluble Zn(II) ions. The proportion of Zn(II) in bentonite and clay increased from 0 to 0.33% and 0.53% respectively, with the proportion of Na decreased in two absorbents. It indicating that the Na is exchanged by Zn(II) in interlayer according to the law of cation exchange. In addition, the decrease in the content of certain alkaline metals,

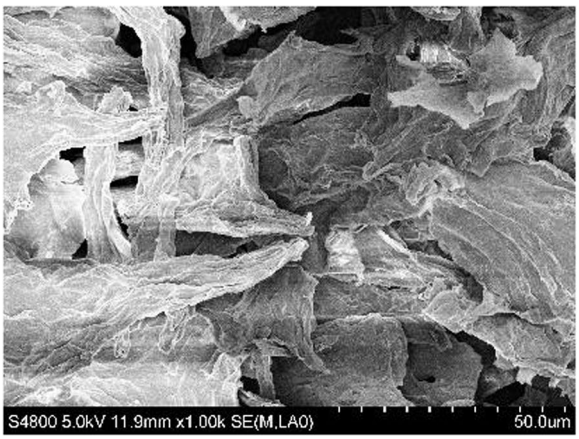

(a) Bentonite

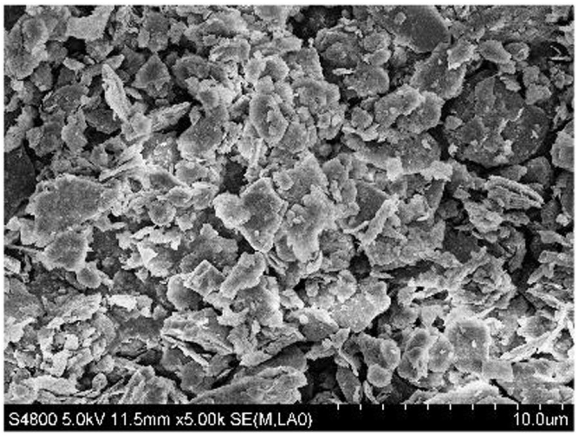

(b) Clay

Fig. 14 The SEM images of bentonite (**a**) and clay (**b**) before Zn(II) adsorption

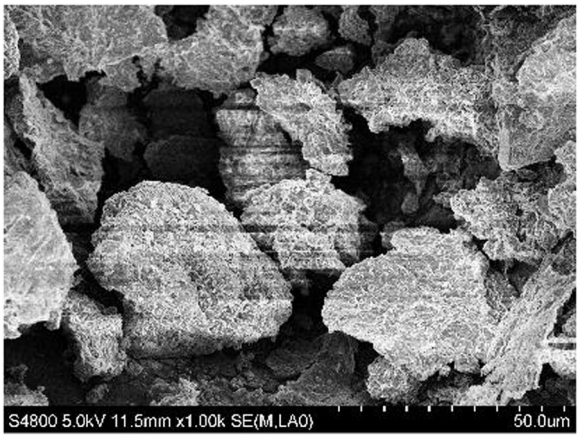

(a) Bentonite

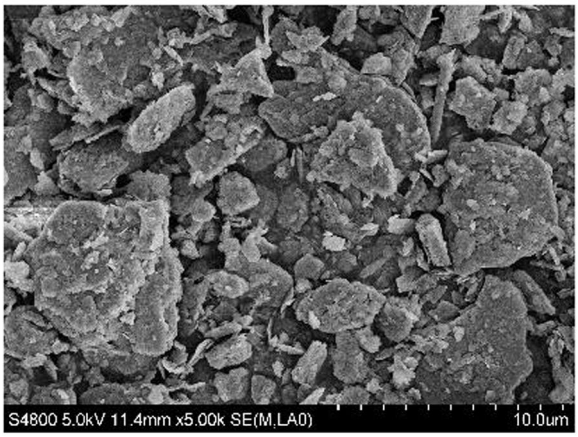

(b) Clay

Fig. 15 The SEM images of bentonite (**a**) and clay (**b**) after Zn(II) adsorption

such as Na and K, confirms the buffer capacity of the two adsorbents described in Sect. "Effect of pH on Zn(II) adsorption".

The functional groups of bentonite and clay before and after adsorption were analyzed by FTIR, as shown in Fig. 16. The bonds at 3445.69–3632.63 cm^{-1} is caused by stretching vibration of hydroxyl on surface of montmorillonite (Ye et al. 2015; Kumar and Lingfa 2020). The band at 1046.48 cm^{-1} is ascribed to the stretching vibration of Si–O in montmorillonite structure (Zazoua et al. 2013), and the bands at 795.41 cm^{-1} and 779.23 cm^{-1} is ascribed to stretching vibration of Si–O–Si in quartz. When the anions are the same and the cations are different, the heavier the cation, the lower the lattice vibrational frequency. The bands at 1046.48 cm^{-1} move to 1043.58 cm^{-1} indicating that the groups on surface of bentonite is change from Si–O–Na to Si–O–Zn after adsorption, which showed that there are some Zn(II)

Table 6 The EDS result of bentonite and clay before and after Zn(II) adsorption

Elements	Content/%			
	Bentonite		Clay	
	Before adsorption	After adsorption	Before adsorption	After adsorption
C	0.88	22.95	4.46	0.71
O	33.93	35.94	44.09	40.05
Na	2.55	0.44	0.69	0.20
Mg	1.41	0.87	2.07	5.60
Al	7.80	5.07	9.88	10.31
Si	22.06	16.83	18.19	12.28
K	0.30	0.20	2.78	0.31
Ca	0.76	1.24	0.76	0.05
Fe	3.33	2.10	5.06	19.81
Zn	0.00	0.33	0.00	0.53

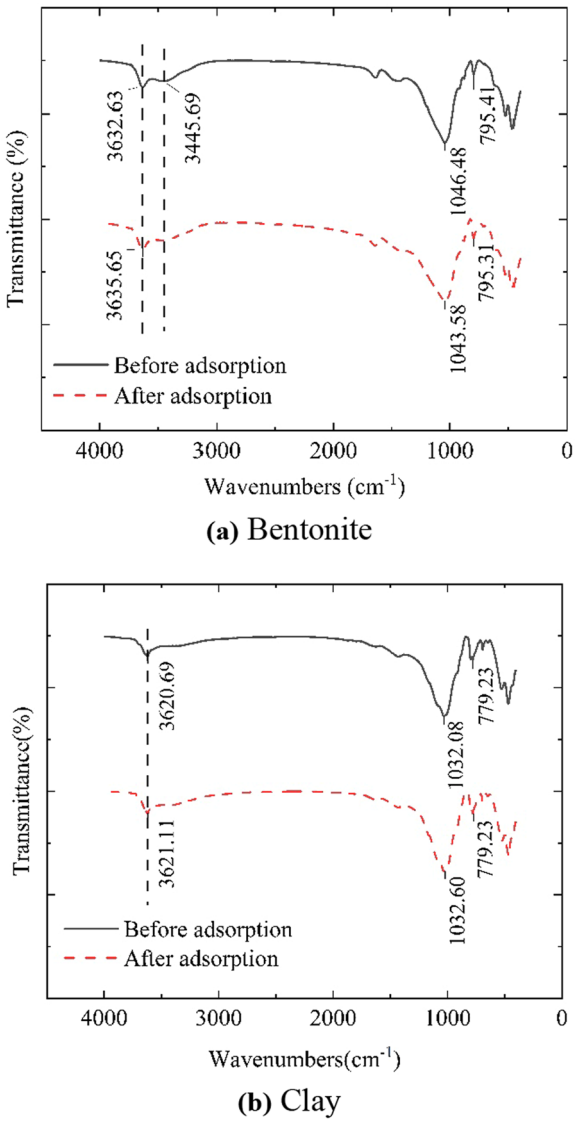

Fig. 16 The FTIR patterns of bentonite (**a**) and clay (**b**) before and after Zn(II) adsorption

ions inside the interlayer space of montmorillonite. The spectrum of clay after adsorption is almost the same as that of original clay, and the functional groups do not change. The band of hydroxyl stretching vibration at 3620.69 cm^{-1} move to 3620.69 cm^{-1}, which may be caused by the coordination of the metal surface.

In summary, the adsorption mechanism of adsorption Zn(II) on bentonite and clay is mainly physical and chemical adsorption (Sahmoune 2018). The physical adsorption is explained by Van der Waals force, which is between adsorbent and adsorbate, and cation exchange (Zou et al. 2019). The chemical adsorption is attributed to the formation of chemical bond on the surface of adsorbents, which is inferred by fixation as outer-sphere cations on the surface of adsorbent and by fixation of hydroxyl cations as inner sphere complexes (Pablo et al. 2011). Then, the Zn(II) adsorption onto bentonite is attributed to pH-independent cation exchange, which is the reason that the adsorption capacity of bentonite does not change with the increase of pH. The Zn(II) adsorption onto clay is mainly attributed to pH-dependent surface complexation on amphoteric surface hydroxyl groups.

In addition, the reason that the Zn(II) adsorption capacity onto bentonite are generally better than that of clay is explained by the different degrees of adsorption. For example, the cation exchange capacity of bentonite is higher than that of clay, and the number of surface exchange sites is greater than that of clay.

Conclusions

Manufacturing in the zinc industry leads to an increase in the proportion of zinc in leachate. Hence, the control of the solute zinc is important. Bentonite has been known as barrier in landfill for effectively removing heavy metals due to its high adsorption capacity and low permeability. In this study, the adsorption performance of bentonite and clay, which come from general landfill in shanghai, China, in different effect factor is investigated by Batch-type adsorption test. The effect factors are included pH, the Na concentration, contact time, the initial concentration of Zn(II) and adsorption temperature, it can be concluded by the following aspects:

1. The pH and Na concentration of solution has a slight impact on the adsorption of Zn(II) onto bentonite, however, the Zn(II) equilibrium adsorption capacity onto clay increased with the increase in pH value and decreased with the increase in Na concentration. It indicating that the adsorption of Zn(II) onto bentonite is pH-independent.
2. The result of adsorption kinetic shows that the adsorption process can be well described by pseudo-second-order, intra-particle diffusion model and Elovih model. The adsorption process of Zn(II) onto bentonite and clay is characterized by both physical and chemical adsorption, and the chemical adsorption is the main rate limiting step of adsorption process. The resulting adsorption isotherm shows a favorable adsorption on bentonite and clay due to the reason that the $1/n$ value ranges from 0.1 to 0.5. In addition, the adsorption of Zn(II) onto bentonite can be happened spontaneously, whereas spontaneous adsorption of Zn(II) is unlikely happened in terms of shanghai clay.

3. The results of SEM, EDS, FTIR indicate that physical adsorption, such as cation exchange and electrostatic interactions, plays as an important role in the adsorption of Zn(II) onto bentonite and shanghai clay.

Author contributions
W-JS designed the experiments and analyzed the data. GGS operated the experiments and prepared data. Q-TT analyzed the data and writes the manuscript. R-DF analyzed the data and supervised manuscript. YT supervised manuscript. All authors read and approved the final manuscript. G-GS Assist in revising the manuscript.

Funding
This study was supported by the National Natural Science Foundation of China (Nos. 41977214, 41572284, 51908121) for the financial supports, and the Natural Science Foundation of Shanghai Province (No. 22ZR1401800), and the Fundamental Research Funds for the Central Universities.

Availability of data and materials
The datasets used or analysed during the current study are available from the corresponding author on reasonable request.

Declarations

Competing interests
The authors declare that they have no competing interests.

Received: 25 July 2023 Accepted: 28 December 2023
Published online: 23 January 2024

References

Ahmed AM, Ayad MI, Eledkawy MA, Darweesh MA, Elmelegy EM (2021) Removal of iron, zinc, and nickel-ions using nano bentonite and its applications on power station wastewater. Heliyon 7:e06315. https://doi.org/10.1016/j.heliyon.2021.e06315

Albadarin AB, Mangwandi C, Al-Muhtaseb AH, Walker GM, Allen SJ, Ahmad MNM (2012) Kinetic and thermodynamics of chromium ions adsorption onto low-cost dolomite adsorbent. Chem Eng J 179:193–202. https://doi.org/10.1016/j.cej.2011.10.080

An N, Zagorščak R, Thomas HR, Gao W (2021) A numerical investigation into the environmental impact of underground coal gasification technology based on a coupled thermal-hydro-chemical model. J Clean Prod 290:125181. https://doi.org/10.1016/j.jclepro.2020.125181

An N, Zagorščak R, Thomas HR (2022a) Transport of heat, moisture, and gaseous chemicals in hydro-mechanically altered strata surrounding the underground coal gasification reactor. Int J Coal Geol 249:103879. https://doi.org/10.1016/j.coal.2021.103879

An N, Zagorščak R, Thomas HR (2022b) Adsorption characteristics of rocks and soils, and their potential for mitigating the environmental impact of underground coal gasification technology: a review. J Environ Manag 305:114390. https://doi.org/10.1016/j.jenvman.2021.114390

Bagherifam S, Brown TC, Fellows CM, Naidu R, Komarneni S (2021) Highly efficient removal of antimonite (Sb(III)) from aqueous solutions by organo-clay and organozeolite: Kinetics and Isotherms. Appl Clay Sci. https://doi.org/10.1016/j.clay.2021.106004

Caporale AG, Violante A (2016) Chemical processes affecting the mobility of heavy metals and metalloids in soil environments. Curr Pollut Rep 2:15–27. https://doi.org/10.1007/s40726-015-0024-y

Chai W, Huang Y, Su S, Han GH, Liu JT, Cao YJ (2017) Adsorption behavior of Zn(II) onto natural minerals in wastewater. A comparative study of bentonite and kaolinite. Physicochem Probl Miner Process 53(1):264–278. https://doi.org/10.5277/ppmp170122

Chang YS, Au PI, Mubarak NM, Khalid M, Jagadish P, Walvekar R, Abdullah EC (2020) Adsorption of Cu(II) and Ni(II) ions from wastewater onto bentonite and bentonite/GO composite. Environ Sci Pollut Res 27:33270–33296. https://doi.org/10.1007/s11356-020-09423-7

Chen YG, He Y, Ye WM, Lin CH, Zhang XF, Ye B (2012) Removal of chromium(III) from aqueous solutions by adsorption on bentonite from Gaomiaozi, China. Environ Earth Sci 67:1261–1268. https://doi.org/10.1007/s12665-012-1569-3

Chen YG, He Y, Ye WM, Jia LY (2015) Competitive adsorption characteristics of Na(I)/Cr(III) and Cu(II)/Cr(III) on GMZ bentonite in their binary solution. J Ind Eng Chem 26:335–339. https://doi.org/10.1016/j.jiec.2014.12.006

Dinh VP, Nguyen PT, Tran MC, Luu AT, Hung NQ, Luu TT, Tuan Kiet HA, Mai XT, Luong TB, Nguyen TL, Ho HTT, Nguyen DK, Pham DK, Hoang AQ, Le VT, Nguyen TC (2022) HTDMA-modified bentonite clay for effective removal of Pb(II) from aqueous solution. Chemosphere 286:131766. https://doi.org/10.1016/j.chemosphere.2021.131766

Elbana TA, Selim HM (2019) Modeling of cadmium and nickel release from different soils. Geoderma 338:78–87. https://doi.org/10.1016/j.geoderma.2018.11.041

Hao W, Pudasainee D, Gupta R, Kashiwabara T, Alessi DS, Konhauser KO (2019) Effect of acidic conditions on surface properties and metal binding capacity of clay minerals. ACS Earth Space Chem 3:2421–2429. https://doi.org/10.1021/acsearthspacechem.9b00166

Huang Z, Liu S, Zhang B, Xu LL, Hu XF (2012) Equilibrium and kinetics studies on the adsorption of Cu(II) from the aqueous phase using a β-cyclodextrin-based adsorbent. Carbohydr Polym 88:609–617. https://doi.org/10.1016/j.carbpol.2012.01.009

Huang B, Yuan Z, Li D, Zheng M, Nie X, Liao Y (2020) Effects of soil particle size on the adsorption, distribution, and migration behaviors of heavy metal(loid)s in soil: a review. Environ Sci Process Impacts 22:1596–1615. https://doi.org/10.1039/d0em00189a

Inyang HI, Onwawoma A, Bae S (2016) The Elovich equation as a predictor of lead and cadmium adsorption rates on contaminant barrier minerals. Soil Tillage Res 155:124–132. https://doi.org/10.1016/j.still.2015.07.013

Jiang MQ, Jin XY, Lu XQ, Chen ZL (2010) Adsorption of Pb(II), Cd(II), Ni(II) and Cu(II) onto natural kaolinite clay. Desalination 252:33–39. https://doi.org/10.1016/j.desal.2009.11.005

Jiang J, Wang YP, Yu M, Li K, Shan YJ, Yan JH (2016) Responses of soil buffering capacity to acid treatment in three typical subtropical forests. Sci Total Environ 563–564:1068–1077. https://doi.org/10.1016/j.scitotenv.2016.04.198

Kumar A, Lingfa P (2020) Physicochemical characterization of sodium bentonite clay and its significance as a catalyst in plastic wastes valorization. Am J Electron Commun 1:6–9. https://doi.org/10.15864/ajec.1202

Liu Z, Zhang Y, Liu B, Zeng L, Xu D, He F, Kong LW, Zhou QH, Wu ZB (2017) Adsorption performance of modified bentonite granular (MBG) on sediment phosphorus in all fractions in the West Lake, Hangzhou, China. Ecol Eng 106:124–131. https://doi.org/10.1016/j.ecoleng.2017.05.042

Mahmoud GA (2013) Adsorption of copper(II), lead(II), and cadmium(II) ions from aqueous solution by using hydrogel with magnetic properties. Chem Mon 144:1097–1106. https://doi.org/10.1007/s00706-013-0957-z

Matouq M, Jildeh N, Qtaishat M, Hindiyeh M, Al Syouf MQ (2015) The adsorption kinetics and modeling for heavy metals removal from wastewater by Moringa pods. J Environ Chem Eng 3:775–784. https://doi.org/10.1016/j.jece.2015.03.027

Maung KN, Lwin CM, Hashimoto S (2019) Assessment of secondary zinc reserves of nations. J Ind Ecol 23:1109–1120. https://doi.org/10.1111/jiec.12847

Musso T, Parolo M, Pettinari G (2019) pH, ionic strength, and ion competition effect on Cu(II) and Ni(II) adsorption by a Na-bentonite used as liner material. Pol J Environ Stud 28:2299–2309. https://doi.org/10.15244/pjoes/84922

Negi P, Mor S, Ravindra K (2018) Impact of landfill leachate on the groundwater quality in three cities of North India and health risk assessment. Environ Dev Sustain 22:1455–1474. https://doi.org/10.1007/s10668-018-0257-1

Niu M, Li G, Cao L, Wang XD, Wang WZ (2020) Preparation of sulphate aluminate cement amended bentonite and its use in heavy metal adsorption. J Clean Prod. https://doi.org/10.1016/j.jclepro.2020.120700

Pablo LD, Lourdes Chávez M, Abatal M (2011) Adsorption of heavy metals in acid to alkaline environments by montmorillonite and Ca-montmorillonite. Chem Eng J 171:1276–1286. https://doi.org/10.1016/j.cej.2011.05.055

Rout GR, Das P (2009) Effect of metal toxicity on plant growth and metabolism: I. Zinc. Sustain Agric. https://doi.org/10.1007/978-90-481-2666-8_53
Sabnavis M, Jagasheth UH, Avachat H, Mishra M (2018) Zinc Industry: the unsung metal of the economy. CARE Ratings: Professional Risk Opinion
Sahmoune MN (2018) Evaluation of thermodynamic parameters for adsorption of heavy metals by green adsorbents. Environ Chem Lett 17:97–704. https://doi.org/10.1007/s10311-018-00819-z
Sihombing JL, Gea S, Pulungan AN, Agusnar H, Wirjosentono B, Hutapea YA (2018) The characterization of Sarulla natural zeolite crystal and its morphological structure. AIP Conf Proc 2049:020062. https://doi.org/10.1063/1.5082467
Song Y, Yang LY, Wang YG, Yu D, Shen JF, Ouyang XK (2019) Highly efficient adsorption of Pb(II) from aqueous solution using amino-functionalized SBA-15/calcium alginate microspheres as adsorbent. Int J Biol Macromol 125:808–819. https://doi.org/10.1016/j.ijbiomac.2018.12.112
Szymanski K, Siebielska I, Janowska B, Sidelko R (2018) Variations in physical and chemical parameters of landfill leachates over time. Desalin Water Treat 117:149–155. https://doi.org/10.5004/dwt.2018.22201
Tohdee K, Kaewsichan L, Asadullah (2018) Enhancement of adsorption efficiency of heavy metal Cu(II) and Zn(II) onto cationic surfactant modified bentonite. J Environ Chem Eng 6:2821–2828. https://doi.org/10.1016/j.jece.2018.04.030
Wang J, Guo X (2020) Adsorption isotherm models: classification, physical meaning, application and solving method. Chemosphere 258:127279. https://doi.org/10.1016/j.chemosphere.2020.127279
Wang Z, Jia M, Li Z, Liu HY, Christie P, Wu LH (2020) Acid buffering capacity of four contrasting metal-contaminated calcareous soil types: changes in soil metals and relevance to phytoextraction. Chemosphere 256:127045. https://doi.org/10.1016/j.chemosphere.2020.127045
Wu Q, Wang J (2020) A thermo-hydro-mechanical coupling analysis for the contaminant transport in a bentonite barrier with variable saturation. Water. https://doi.org/10.3390/w12113114
Wu T, Geng ZL, Feng ZY, Pan GX, Shen Q (2022) Diffusion of Re(VII), Se(IV) and Cr(VI) in compacted GMZ bentonite. J Radioanal Nucl Chem 331:2311–2317. https://doi.org/10.1007/s10967-022-08278-1
Xia M, Chen Z, Li Y, Li CH, Ahmad NM, Cheema WA, Zhu SM (2019) Removal of Hg(II) in aqueous solutions through physical and chemical adsorption principles. RSC Adv 9:20941–20953. https://doi.org/10.1039/c9ra01924c
Xu H, Hu X, Chen YH, Li Y, Zhang RQ, Tang CF, Hu X (2021) Cd(II) and Pb(II) absorbed on humic acid-iron-pillared bentonite: Kinetics, thermodynamics and mechanism of adsorption. Colloids Surf A Physicochem Eng Asp. https://doi.org/10.1016/j.colsurfa.2020.126005
Yang Y, Narayanan Nair AK, Sun S (2019) Layer charge effects on adsorption and diffusion of water and ions in interlayers and on external surfaces of montmorillonite. ACS Earth Space Chem 3:2635–2645. https://doi.org/10.1021/acsearthspacechem.9b00236
Yao QX, Xie JJ, Liu JX, Kang HM, Liu Y (2014) Adsorption of lead ions using a modified lignin hydrogel. J Polym Res. https://doi.org/10.1007/s10965-014-0465-9
Ye W, Zhao B, Gao H, Huang JJ, Zhang XL (2015) Preparation of highly efficient and stable Fe, Zn, Al-pillared montmorillonite as heterogeneous catalyst for catalytic wet peroxide oxidation of Orange II. J Porous Mater 23:301–310. https://doi.org/10.1007/s10934-015-0082-y
Yuan L, Liu Y (2013) Removal of Pb(II) and Zn(II) from aqueous solution by ceramisite prepared by sintering bentonite, iron powder and activated carbon. Chem Eng J 215–216:432–439. https://doi.org/10.1016/j.cej.2012.11.016
Zazoua A, Kazane I, Khedimallah N, Dernane C, Errachid A, Jaffrezic Renault N (2013) Evidence of ammonium ion-exchange properties of natural bentonite and application to ammonium detection. Mater Sci Eng C 33:5084–5089. https://doi.org/10.1016/j.msec.2013.09.005
Zhang HB, Tong ZF, Wei TY, Tang YK (2011) Removal characteristics of Zn(II) from aqueous solution by alkaline Ca-bentonite. Desalination 276:103–108. https://doi.org/10.1016/j.desal.2011.03.026
Zhang H, Omer AM, Hu ZH, Yang LY, Ji C, Ouyang XK (2019) Fabrication of magnetic bentonite/carboxymethyl chitosan/sodium alginate hydrogel beads for Cu(II) adsorption. Int J Biol Macromol 135:490–500. https://doi.org/10.1016/j.ijbiomac.2019.05.185
Zou CL, Jiang W, Liang JY, Sun XH, Guan YY (2019) Removal of Pb(II) from aqueous solutions by adsorption on magnetic bentonite. Environ Sci Pollut Res 26:1315–1322. https://doi.org/10.1007/s11356-018-3652-0

Publisher's Note